

## Supporting Information for

# A Novel Cu(I)-5-nitropyridine-2-thiol Cluster with NIR Emission: Structural and Photophysical Characterization

*Khaled Hassanein,<sup>a</sup> Chiara Cappuccino,<sup>b</sup> Marianna Marchini,<sup>b</sup> Elisa Bandini,<sup>a</sup> Meganne Christian,<sup>c</sup>*

*Vittorio Morandi,<sup>c</sup> Filippo Monti,<sup>a\*</sup> Lucia Maini,<sup>b\*</sup> Barbara Ventura<sup>a\*</sup>*

<sup>a</sup> Istituto per la Sintesi Organica e la Fotoreattività (ISOF), Consiglio Nazionale delle Ricerche

(CNR), Via P. Gobetti 101, 40129 Bologna, Italy. email: [filippo.monti@isof.cnr.it](mailto:filippo.monti@isof.cnr.it);

[barbara.ventura@isof.cnr.it](mailto:barbara.ventura@isof.cnr.it)

<sup>b</sup> Dipartimento di Chimica “G. Ciamician”, Università di Bologna, Via F. Selmi 2, 40126 Bologna,

Italy. email: [l.maini@unibo.it](mailto:l.maini@unibo.it)

<sup>c</sup> Istituto per la Microelettronica e Microsistemi (IMM) Sede di Bologna, Consiglio Nazionale delle

Ricerche (CNR), Via P. Gobetti 101, 40129 Bologna, Italy.



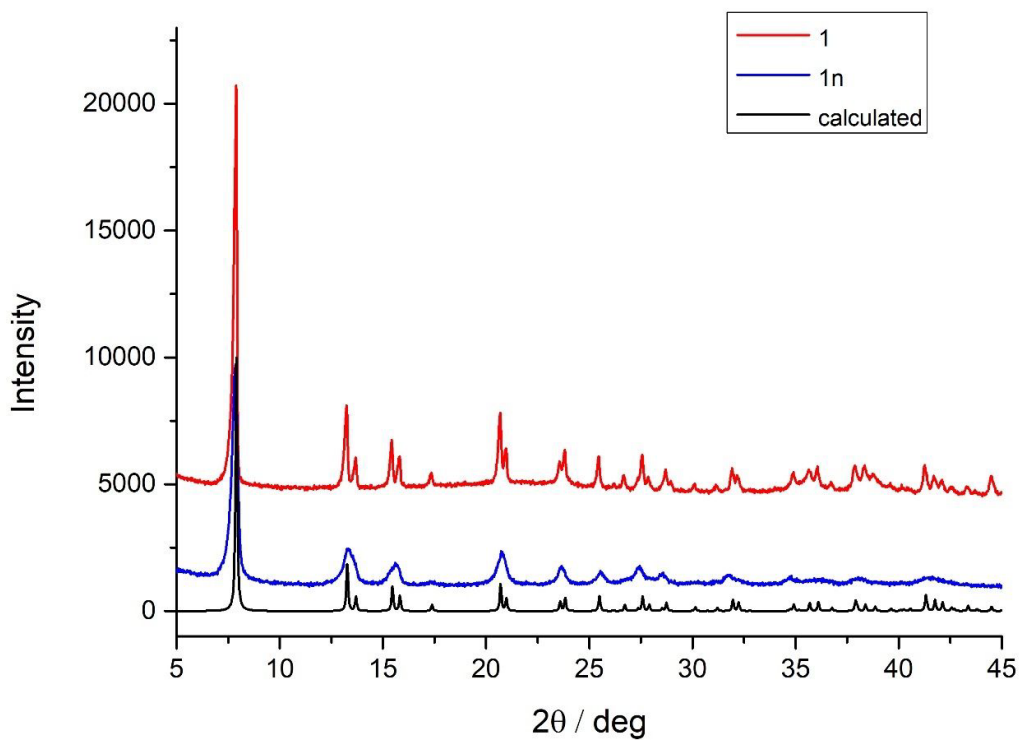


**Figure S1:** XRPD patterns of **1**, **1n** and the calculated pattern of **1**.

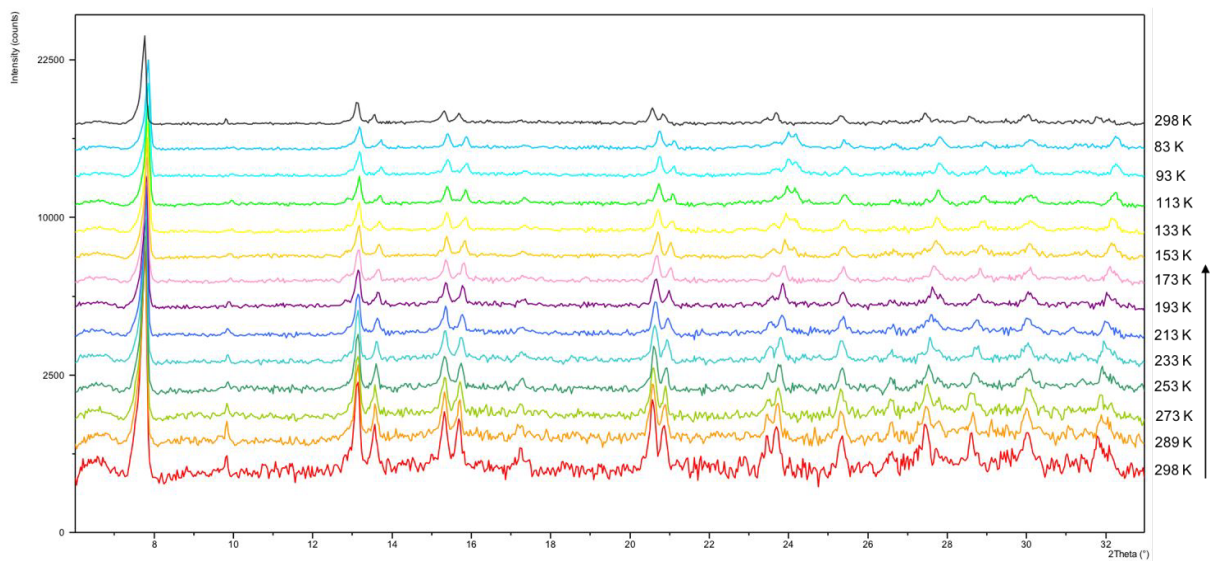


**Figure S2.** Variable-temperature X-ray powder diffraction analysis of compound **1**. Powder pattern profiles measured *in situ*, color changes of the sample cooled down from 298 K (red line, bottom) to 83 K. At the end of the measurement, the sample was heated up to 298 K again (black line, top). No phase transition is observed, the shift of the peaks is due to thermal contraction.

**Table S1.** Crystallographic data of compound **1** at room temperature.

Chemical formula	$C_{30}H_{18}Cu_6N_{12}O_{12}S_6$
Formula Mass	1312.22 g/mol
Temperature	RT
Crystal System	Trigonal
Space Group	R-3
a/Å	22.3832(12)
b/Å	22.3832(12)
c/Å	7.0996(4)
$\alpha/^\circ$	90
$\beta/^\circ$	90
$\gamma/^\circ$	120
Volume/ Å <sup>3</sup>	3080.41
R(int)	0.035
R1	0.0342
R2 (all data)	0.0530
Chi <sup>2</sup>	1.013

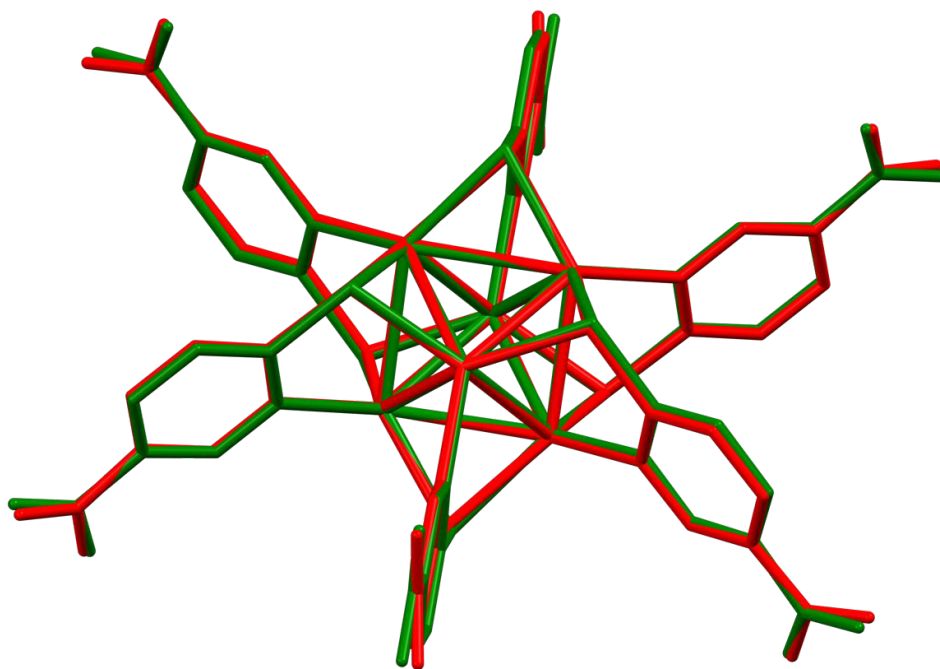
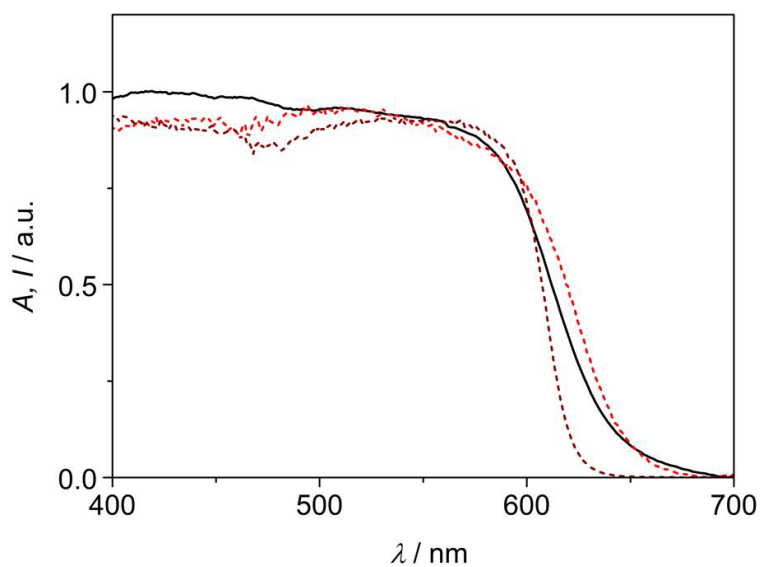


**Figure S3.** Comparison between the experimental X-ray structure of complex **1** (red) and the one optimised by DFT methods (green). The structural overlap is obtained by minimizing the root-mean-square deviation (RMSD) of all the atomic positions except hydrogen atoms.

**Table S2.** Comparison between key geometrical parameters of complex **1** obtained from X-ray diffraction crystallography and DFT optimizations in vacuum.

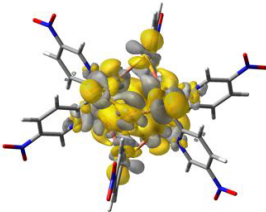
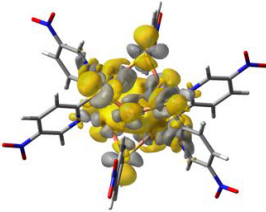
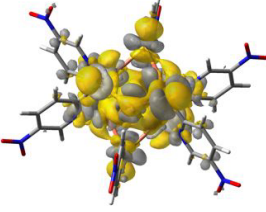
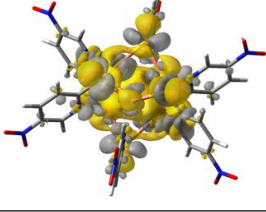
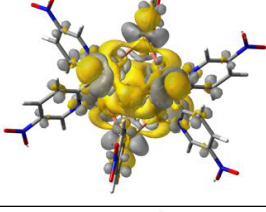
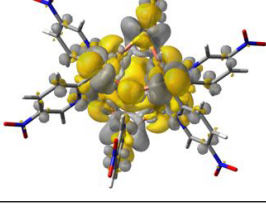
	X-ray data [S <sub>6</sub> ]	DFT data ground state [D <sub>3d</sub> ]	U-DFT data lowest triplet state [C <sub>s</sub> ]
Distances [Å]			
Cu–Cu	2.819	2.757	2.582–2.438–2.582 2.596–2.568–2.596
Cu–Cu'	2.792	2.751	2.635–2.620–2.563
Cu–S	2.249–2.250	2.284	2.340–2.363–2.371 2.330–2.341–2.338
Cu–N	2.053	2.079	2.009–2.069–2.009 2.099–2.102–2.099
C–S	1.736	1.750	1.751–1.751–1.751 1.746–1.747–1.746
Angles [°]			
Cu–Cu–Cu	60.00	60.00	61.83–56.34–61.83 60.35–59.29–60.35
Cu–Cu'–Cu	60.66	60.12	58.86–56.80–58.86 60.10–58.33–60.10
Cu–Cu–Cu'	59.67	59.94	60.86–61.60–60.28 60.84–61.03–58.87
Cu–S–Cu	77.62	74.22	66.59–61.88–66.59 67.38–66.87–67.38
S–Cu–Cu	51.19–51.21	52.89	56.28–59.06–57.13 56.26–56.56–56.36
S–Cu–Cu'	79.99–80.00	82.53	86.91–87.31–86.79 84.69–85.77–83.37
N–Cu–Cu	142.00–143.38	142.25	143.87–141.25–148.17 143.98–140.77–142.82
N–Cu–Cu'	86.50–87.34	86.06	87.00–88.28–91.25 85.37–86.28–87.84
Cu–N–C	120.68	122.38	121.25–123.14–121.25 124.23–123.50–124.23
Cu–S–C	105.94–106.49	104.27	101.35–100.46–101.09 102.45–100.80–101.75
N–Cu–S	110.22–111.78	110.91	110.27–102.64–106.69 109.63–106.18–106.55
S–C–N	119.61	119.70	120.45–120.51–120.45 120.92–120.67–120.92
Dihedrals [°]			
Cu–N–C–S	1.30	0.00	2.08–0.00–2.08 2.40–0.00–2.40
Cu–Cu'–S–C	44.27–44.94	43.40	40.50–40.95–38.71 40.36–42.36–38.14
Cu–Cu–Cu–S	25.30	27.58	31.15–32.28–31.56

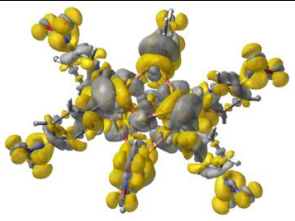
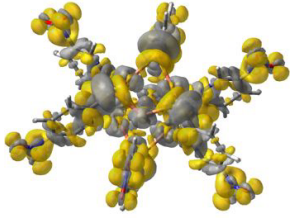
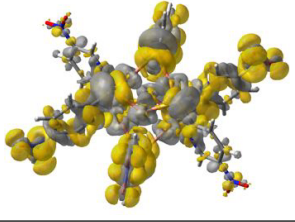
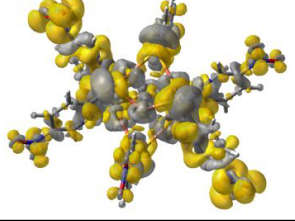
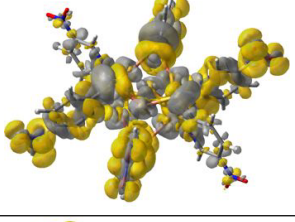
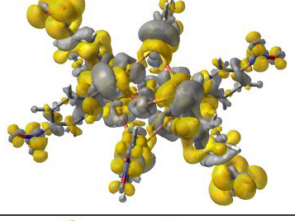
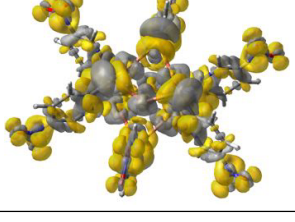
			27.83–30.09–27.95
Cu–Cu–Cu–S	148.00	146.02	143.52–144.74–143.52 147.96–145.36–147.96
Cu'–Cu'–Cu'–N	138.46–140.02	138.22	137.18–144.57–150.76 136.43–138.80–141.52
Cu–Cu–Cu–Cu'	54.33	54.66	55.09–55.54–55.79 54.48–55.59–56.28
Cu–Cu–Cu–Cu'	109.74	109.52	109.32–110.07–109.32 108.09–109.14–108.09
py–NO <sub>2</sub>	10.45	0.00	0.23–0.00–0.23 0.04–0.00–0.04



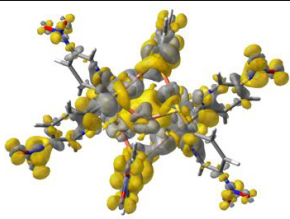
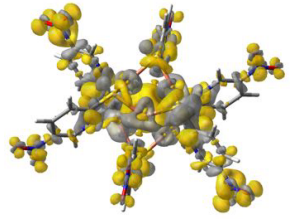
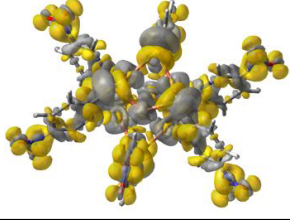
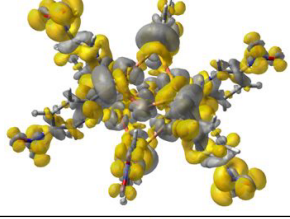
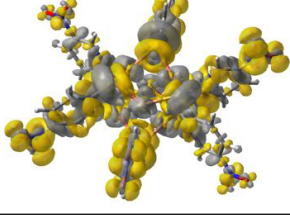
**Figure S4.** Arbitrarily scaled absorption spectrum (black solid), room temperature excitation spectrum (red dash,  $\lambda_{\text{em}} = 768$  nm), low temperature excitation spectrum (brown dash,  $\lambda_{\text{em}} = 823$  nm) of a powder sample of **1** obtained from bulk solution.

**Table S3.** The lowest 18 singlet vertical excitation for compound **1** in vacuum. Density differences are computed as  $\rho_{S_n} - \rho_{S_0}$  using relaxed excited-state densities and the ground-state SCF one. Isodensities = + 0.0004 (yellow, electron) and - 0.0004 e bohr<sup>-3</sup> (gray, hole). The symmetry of each excited state (and molecular orbital) is given accordingly to the ground-state D<sub>3d</sub> point group.

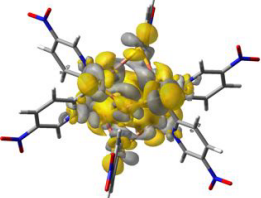
	Transition energy [eV (nm)] <i>oscillator strength</i>	Density difference ( $\rho_{S_n} - \rho_{S_0}$ )	Molecular-orbital contribution	Nature
$S_0 \rightarrow S_1$ (E <sub>u</sub> )	2.42 (512) <i>f</i> = 0.092		H-1 → L+4 (e <sub>u</sub> ) (a <sub>1g</sub> ) 96.1%	cluster centered
$S_0 \rightarrow S_2$ (E <sub>u</sub> )	2.42 (512) <i>f</i> = 0.092		H → L+4 (e <sub>u</sub> ) (a <sub>1g</sub> ) 96.1%	cluster centered
$S_0 \rightarrow S_3$ (E <sub>g</sub> )	2.43 (511) <i>f</i> = 0.000		H-4 → L+4 (e <sub>g</sub> ) (a <sub>1g</sub> ) 97.6%	cluster centered
$S_0 \rightarrow S_4$ (E <sub>g</sub> )	2.43 (511) <i>f</i> = 0.000		H-3 → L+4 (e <sub>g</sub> ) (a <sub>1g</sub> ) 97.6%	cluster centered
$S_0 \rightarrow S_5$ (A <sub>2g</sub> )	2.49 (499) <i>f</i> = 0.000		H-2 → L+4 (a <sub>2g</sub> ) (a <sub>1g</sub> ) 97.5%	cluster centered
$S_0 \rightarrow S_6$ (A <sub>1u</sub> )	2.80 (443) <i>f</i> = 0.000		H-5 → L+4 (a <sub>1u</sub> ) (a <sub>1g</sub> ) 93.1%	cluster centered

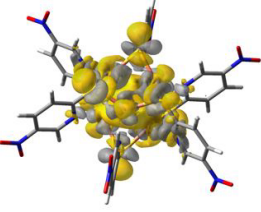
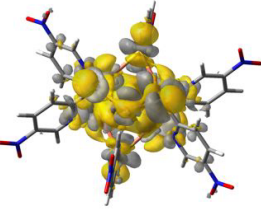
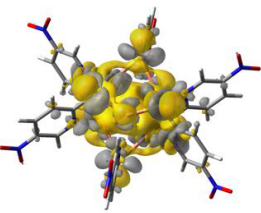
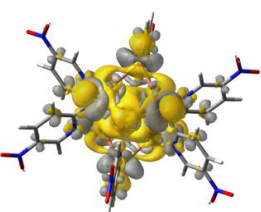
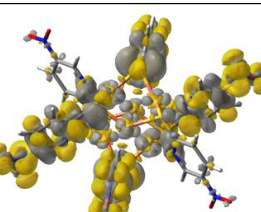
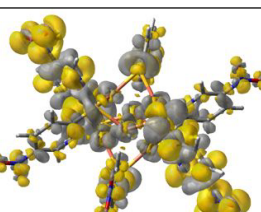
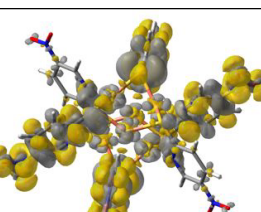
$S_0 \rightarrow S_7$ ( $E_u$ )	2.83 (438) $f = 0.000$		highly multiconfigurational character	charge transfer from core (mainly S) to nitropyridines
$S_0 \rightarrow S_8$ ( $E_g$ )	2.83 (438) $f = 0.000$		highly multiconfigurational character	charge transfer from core (mainly S) to nitropyridines
$S_0 \rightarrow S_9$ ( $E_u$ )	2.88 (431) $f = 0.000$		highly multiconfigurational character	charge transfer from core (mainly S) to nitropyridines
$S_0 \rightarrow S_{10}$ ( $E_u$ )	2.88 (431) $f = 0.000$		highly multiconfigurational character	charge transfer from core (mainly S) to nitropyridines
$S_0 \rightarrow S_{11}$ ( $E_g$ )	2.89 (430) $f = 0.001$		highly multiconfigurational character	charge transfer from core (mainly S) to nitropyridines
$S_0 \rightarrow S_{12}$ ( $E_g$ )	2.89 (430) $f = 0.001$		highly multiconfigurational character	charge transfer from core (mainly S) to nitropyridines
$S_0 \rightarrow S_{13}$ ( $E_u$ )	2.93 (423) $f = 0.000$		highly multiconfigurational character	charge transfer from core (mainly S) to nitropyridines

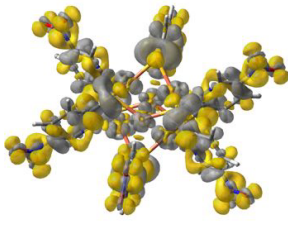
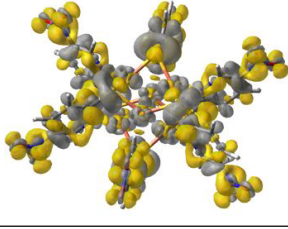


$S_0 \rightarrow S_{14}$ ( $E_g$ )	2.94 (422) $f = 0.000$		highly multiconfigurational character	mixed cluster centered and charge transfer nature
$S_0 \rightarrow S_{15}$ ( $E_g$ )	2.94 (422) $f = 0.000$		highly multiconfigurational character	mixed cluster centered and charge transfer nature
$S_0 \rightarrow S_{16}$ ( $E_g$ )	2.94 (422) $f = 0.015$		highly multiconfigurational character	charge transfer from core (mainly S) to nitropyridines
$S_0 \rightarrow S_{17}$ ( $E_g$ )	2.96 (419) $f = 0.094$		highly multiconfigurational character	charge transfer from core (mainly S) to nitropyridines
$S_0 \rightarrow S_{18}$ ( $E_g$ )	2.96 (419) $f = 0.094$		highly multiconfigurational character	charge transfer from core (mainly S) to nitropyridines

**Table S4.** The lowest 14 triplet vertical excitation for compound **1** in vacuum. Density differences are computed as  $\rho_{T_n} - \rho_{S_0}$  using relaxed excited-state densities and the ground-state SCF one. Isodensities = + 0.0004 (yellow, electron) and - 0.0004 e bohr<sup>-3</sup> (gray, hole). The symmetry of each excited state (and molecular orbital) is given accordingly to the ground-state  $D_{3d}$  point group.

	Transition energy [eV (nm)]	Density difference ( $\rho_{T_n} - \rho_{S_0}$ )	Molecular-orbital contribution	Nature
$S_0 \rightarrow T_1$ ( $E_u$ )	2.27 (547)		H-1 → L+4 ( $e_u$ ) (a <sub>1g</sub> ) 96.8%	cluster centered

$S_0 \rightarrow T_2$ ( $E_u$ )	2.27 (547)		H $\rightarrow$ L+4 ( $e_u$ ) ( $a_{1g}$ ) 96.8%	cluster centered
$S_0 \rightarrow T_3$ ( $E_g$ )	2.35 (528)		H-4 $\rightarrow$ L+4 ( $e_g$ ) ( $a_{1g}$ ) 97.1%	cluster centered
$S_0 \rightarrow T_4$ ( $E_g$ )	2.35 (528)		H-3 $\rightarrow$ L+4 ( $e_g$ ) ( $a_{1g}$ ) 97.1%	cluster centered
$S_0 \rightarrow T_5$ ( $A_{2g}$ )	2.41 (514)		H-2 $\rightarrow$ L+4 ( $a_{2g}$ ) ( $a_{1g}$ ) 96.8%	cluster centered
$S_0 \rightarrow T_6$ ( $E_g$ )	2.60 (477)		highly multiconfigurational character	charge transfer from core (mainly S) to nitropyridines
$S_0 \rightarrow T_7$ ( $E_g$ )	2.60 (477)		highly multiconfigurational character	charge transfer from core (mainly S) to nitropyridines
$S_0 \rightarrow T_8$ ( $E_u$ )	2.60 (477)		highly multiconfigurational character	charge transfer from core (mainly S) to nitropyridines

$S_0 \rightarrow T_9$ ( $E_u$ )	2.60 (477)		highly multiconfigurational character	charge transfer from core (mainly S) to nitropyridines
$S_0 \rightarrow T_{10}$ ( $E_g$ )	2.61 (476)		highly multiconfigurational character	charge transfer from core (mainly S) to nitropyridines
$S_0 \rightarrow T_{11}$ ( $E_u$ )	2.61 (474)		highly multiconfigurational character	charge transfer from core (mainly S) to nitropyridines

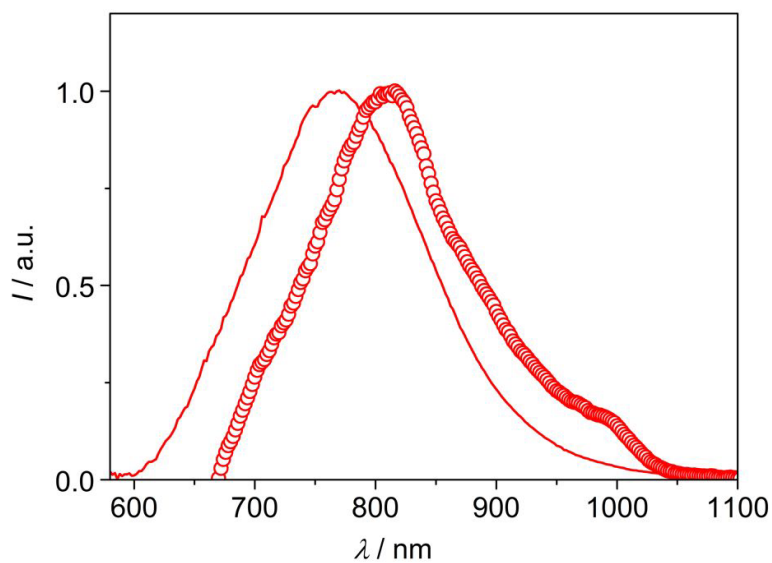


**Figure S5.** Normalized corrected emission spectra of **1** (as powder) from bulk solution (solid line) and from fast precipitation conditions (**1n**, open circles).  $\lambda_{\text{exc}} = 450$  nm.

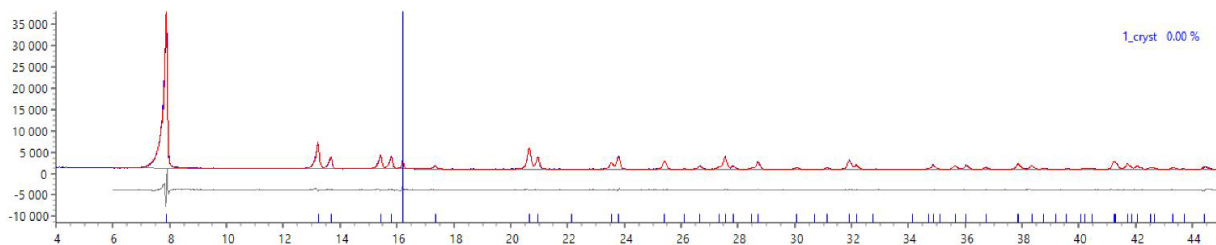


**Figure S6.** Pawley refinement on the powder pattern of the sample **1** to determine the average crystal size with the Scherrer formula (crystal shape factor =1). An extra peak due to the sample holder is observed at  $2\theta = 16.21^\circ$ . Experimental pattern in blue, calculated pattern in red, difference plot in gray. The refinement converged at  $R_{wp} = 4.53\%$ .

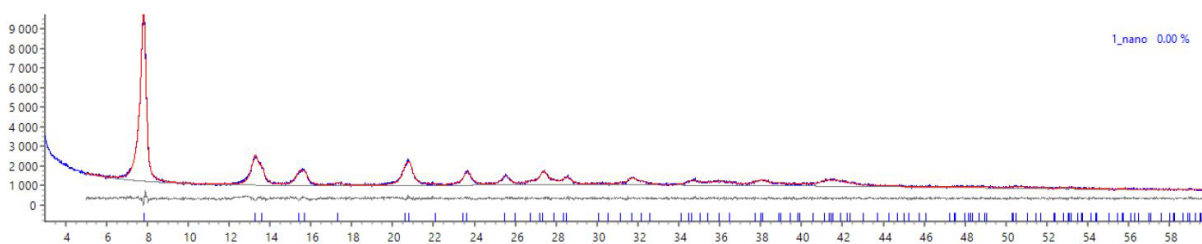


**Figure S7.** Pawley refinement on the powder pattern of the sample **1n** to determine the average crystal size with the Scherrer formula (crystal shape factor =1). Experimental pattern in blue, calculated pattern in red, difference plot in gray. The refinement converged at  $R_{wp} = 2.81\%$ .